Acta Metallurgica, Vol. 28, pp. 1103 to 1114

0001–6160/80/0801-1103$02.00/0

THE LOWER BAINITE TRANSFORMATION AND THE SIGNIFICANCE OF CARBIDE PRECIPITATION

H. K. D. H. BHADESHIA

Department of Metallurgy and Materials Science, University of Cambridge, Cambridge CB2 3QZ, England

(*Received* 22 *November* 1979; *in revised form* 28 *January* 1980)

Abstract—The nature and significance of carbide precipitation accompanying the lower bainite transformation in steels has been examined. It is found that lower bainitic cementite nucleates and grows from within supersaturated ferrite, and that such precipitation is strongly inconsistent with the concept of 'interphase precipitation' at the α/γ transformation interface. Crystallographic determinations suggest that the lattice invariant shear of lower bainite may not be directly responsible for the occurrence of the characteristic single carbide variant. It is suggested that it is the transformation strain associated with a lower bainite platelet that stimulates the development of a particular carbide variant which is compatible with the relief of this strain. The transition temperature from upper to lower bainite has been tentatively rationalised on thermodynamic grounds and in the context of the B_s and M_s temperatures. It seems that the appearance of epsilon carbide in some lower bainites but cementite in others can be understood in terms of a theory of martensite tempering due to Kalish and Cohen.

Résumé—Nous avons examiné la nature et la signification de la précipitation de carbure qui accompagne la transformation bainitique inférieure dans les aciers. Nous avons trouvé que la cémentite bainitique inférieure germe et croît à partir de la ferrite sursaturée, et qu'une telle précipitation est en profond désaccord avec le concert de 'précipitation interphase' à l'interface de la transformation α/γ. Les déterminations cristallographiques donnent à penser que le cisaillement à réseau invariant de la bainite inférieure ne serait pas directement responsable de l'apparition de l'unique variante de carbure. Nous pensons que c'est la déformation de transformation associée à une plaquette de bainite inférieure qui favorise le développement de la variante particulière de carbure qui est compatible avec le relâchement de cette déformation. Nous avons essayé de rationaliser la température de transition de la bainite supérieure à la bainite inférieure, sur des bases thermodynamiques et dans le cadre des températures B_s et M_s. Il semble que l'on puisse comprendre l'apparition de carbure epsilon dans certaines bainites inférieures et de cémentite dans d'autres, à partir de la théorie de la martensite de Kalish et Cohen.

Zusammenfassung—Bedeutung und Natur der Karbidausscheidung, die die untere Bainitumwandlung in Stählen begleitet, wurden untersucht. Es wird gefunden, daß der untere bainitische Cementit sich in dem übersättigten Ferrit ausbildet und wächst. Diese Art der Ausscheidung ist nicht verträglich mit dem Konzept der 'Grenzflächenausscheidung' an der α/γ-Umwandlungsphasengrenze. Kristallografische Bestimmungen legen nahe, daß die gitterinvariante Scherung des unteren Bainits nicht unmittelbar verantwortlich ist für das Auftreten der charakteristischen, einzigen Karbidvariante. Es wird vorgeschlagen, daß die mit den Bainitplatten zusammenhängenden Umwandlungsverzerrungen die Entwicklung einer solchen Variante bestärken, welche diese Verzerrungen abbauen kann. Die Übergangstemperatur vom oberen zum unteren Bainit wurde versuchsweise thermodynamisch und mit den B_s- und M_s-Temperaturen beschrieben. Es scheint, daß das Auftreten von Epsilon-Karbid in einigen unteren Bainiten, jedoch von Cementit in anderen, mit einer Theorie der Martensithärtung von Kalish und Cohen verstanden werden kann.

INTRODUCTION

The lower bainite transformation in steels results in the formation of a non-lamellar aggregate of ferrite and carbides such that the post-transformation microstructure exhibits a dispersion of plate-like carbides within lenticular ferrite grains [1, 2]. The carbide particles usually precipitate in a single crystallographic orientation such that their habit plane is inclined at about 60° to the plate axis. In some cases, several variants have been observed [3, 4] although the 60° variant still tends to dominate.

Matas and Hehemann [5] first suggested that the initial carbide in hypoeutectoid steels is epsilon carbide, which is subsequently replaced by cementite. Since then, several investigators [6–10], have reported the detection of epsilon carbide in association with lower bainite. On the other hand, in a medium carbon steel, Bhadeshia and Edmonds [3] identified the initial lower bainitic carbide to be cementite despite the high silicon content of the steel used. Silicon is expected to favour the precipitation of epsilon carbide by retarding the formation of cementite [11–13]. It should also be noted that epsilon carbide is not found in low-carbon martensitic steels following appropriate low temperature tempering treatments [14–16]. These observations tend to suggest [3] that the metastable eutectoid transformation ($\gamma \rightleftharpoons \alpha + \epsilon$) proposed in order to rationalise the transition from upper to lower bainite [10] may not exist; if such a transformation

does exist, it cannot be considered as a general phenomenon and hence cannot explain the change from upper to lower bainite. Furthermore, the metastable eutectoid concept requires the eutectoid invariant temperature to be about 350°C, fairly independently of steel composition [10]. However, in many cases [17, 18], the transition from upper to lower bainite occurs at very much higher temperatures.

For upper bainite, it has been shown [3] that the precipitation of cementite from carbon-enriched residual austenite is a secondary process, not essential to the mechanism of formation of bainitic ferrite except in the trivial sense that any precipitation from austenite will deplete its carbon content, thereby promoting further transformation. However, with lower bainite, the precise role of intra-ferrite carbides in the transformation sequence is not clear. The observation [3] that in a high-silicon steel carbide precipitation accompanied only the lower bainite transformation (and not the upper bainite or the martensite transformation) suggests that carbide precipitation in lower bainitic ferrite may have a critical role to play in the transformation mechanism itself. However, before this issue can be tackled, it is necessary to resolve whether lower bainitic carbides precipitate from a supersaturated ferrite matrix, or whether such precipitation can be described as 'interphase precipitation' [19] of the type observed [20] with the high temperature proeutectoid ferrite transformations in alloy steels. In the latter reaction the carbides are envisaged to nucleate at a sessile austenite/ferrite interface (the transformation propagating only by the movement of disordered ledges along this interface) such that the penetration of the carbides into austenite is very much greater than that into ferrite [21]. Aaronson *et al.* [21] have developed a quantitative theory for interphase precipitation and this had led them to conclude that the prolonged debate as to whether bainitic carbides nucleate in austenite or in ferrite is irrelevant, since they deduced that interphase boundary precipitates must necessarily nucleate in both phases. However, the application of their theory to bainitic carbides is unjustified since it is based on the prior assumption that such carbides nucleate at the transformation interface, and do not form within the bainitic ferrite *after* the passage of the transformation interface.

In a silicon steel, lower bainitic carbide precipitation has been shown to be consistent solely with precipitation from supersaturated ferrite [3]. Indeed, in this particular case where substantial quantities of austenite were retained, direct imaging showed the absence of any carbide growth in the austenite. Recalling that for this steel several lower bainitic carbide variants arise, it would be useful to extend these results to the case where only a single variant apparently arises.

Crystallographic observations have often been used to deduce the nucleation and growth sites of bainitic carbides. The ingenious analysis of Shackleton and Kelly [22, 23] supports the hypothesis that lower bainitic carbides originate from supersaturated ferrite, but has been criticised as indirect [19] since it did not involve any austenite (which could not be retained at ambient temperature in the steels used). Another analysis [9] indicated support for the interphase precipitation theory but did not involve simultaneous three phase crystallography and the final results (as far as the lower bainite experiments are concerned) were indirectly deduced using separately determined austenite/ferrite and ferrite/carbide orientation relationships. Srinivasan and Wayman [4] first conducted a direct three phase crystallographic analysis, but their evidence is weakly based in the sense that the electron diffraction pattern analysed contained only one austenite reflection.

The purposes of the present investigation can be summarised as follows:

(a) To resolve the role of lower bainitic carbides with respect to the transformation mechanism.

(b) To resolve the nucleation and growth sites of lower bainitic carbides.

(c) To establish the three phase crystallography of conventional lower bainite, i.e. of the single variant type.

(d) To attempt to rationalise the transition from upper to lower bainite.

EXPERIMENTAL PROCEDURE

The experimental alloy used was prepared from high-purity base materials as a 20 kg vacuum induction melt. The ingot was forged and hot rolled to 10 mm diameter rod, homogenised and finally, hot swaged to 3 mm dia. rod. The final composition was Fe–0.30C–4.08Cr.

This particular alloy was chosen because it exhibits a typical lower bainitic microstructure and also has adequate hardenability to avoid the proeutectoid ferrite reactions. Additionally, the alloy allows the retention of austenite at room temperature.

Austenitising treatments (1100°C for 10 min) were carried out with the specimens protected not only by a dynamic pure argon atmosphere but also a proprietary coating compound. Subsequent isothermal heat treatments were carried out by quenching the specimens into a molten-tin bath covered with a layer of active charcoal.

Thin foil specimens for transmission electron microscopy were prepared from 0.25 mm thick discs slit from the heat-treated 3 mm dia. rod under conditions of flood lubrication. The discs were subsequently thinned and electropolished in a twin-jet polishing unit using a 5% perchloric acid, 25% glycerol and 70% ethanol mixture at room temperature and 55 volts. The foils were examined in a Philips EM300 transmission electron microscope operated at 100 kV.

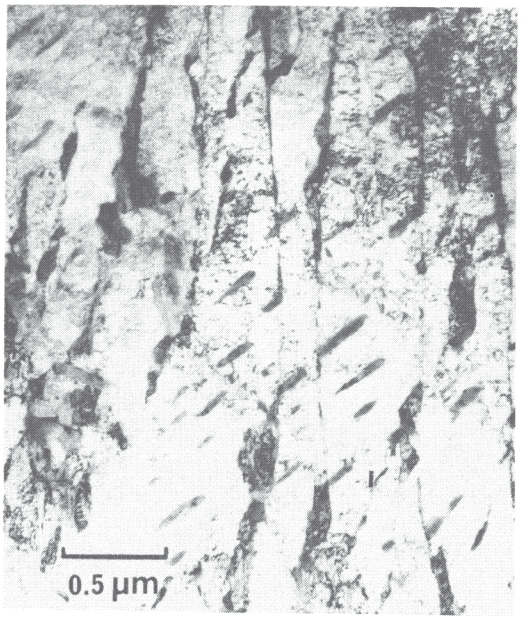

Fig. 1. Typical lower bainitic microstructure following isothermal transformation at 435°C for 10 min.

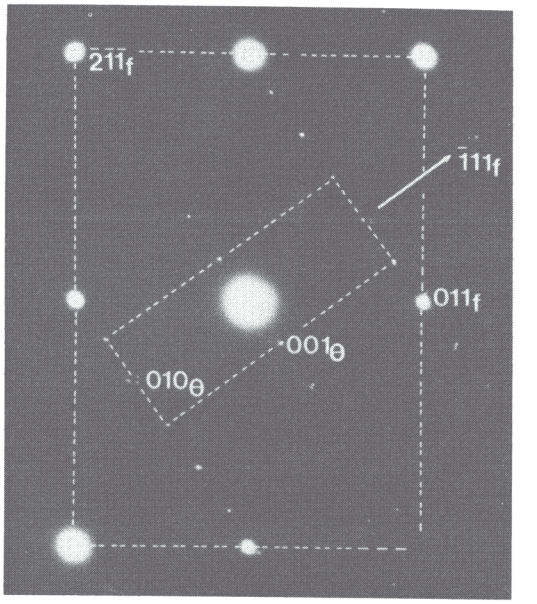

Fig. 2. Electron diffraction pattern illustrating the Bagaryatski orientation relationship between lower bainitic cementite and ferrite.

RESULTS AND DISCUSSION

General observations

Isothermal transformation at 435°C for 10 min gave a typical lower bainitic microstructure of lenticular ferrite platelets containing cementite particles (Fig. 1). The cementite particles precipitated in a single variant of the Bagaryatski [24] orientation relationship, i.e.

$$[100]_\theta \| [0\bar{1}1]_\alpha$$
$$[010]_\theta \| [1\bar{1}\bar{1}]_\alpha$$
$$[001]_\theta \| [211]_\alpha.$$

A typical electron diffraction pattern illustrating this relationship is presented in Fig. 2.

Retained austenite was readily detected between the ferrite platelets and was usually present as thick films (up to 4000 A° thick), Fig. 3. The ability to retain such films of austenite is thought to be due to the limited partitioning of carbon into residual austenite following the formation of supersaturated lower bainitic ferrite [3].

It should be noted that even for the shortest isothermal transformation times used (40 s at 435°C, 10 s at 355°C), epsilon carbide could not be detected.

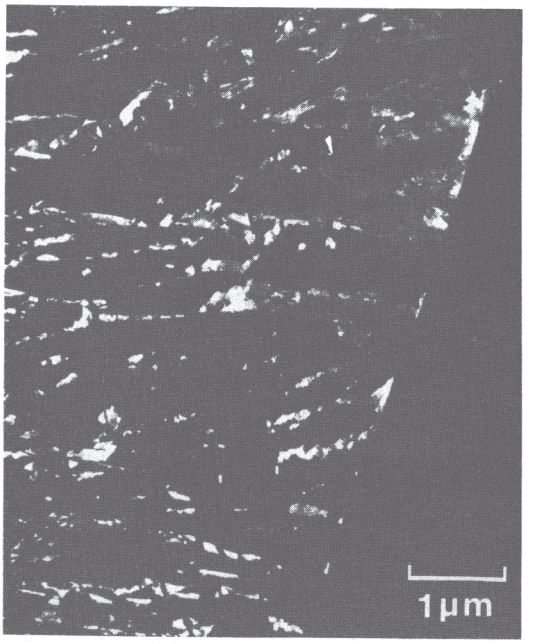

(a)

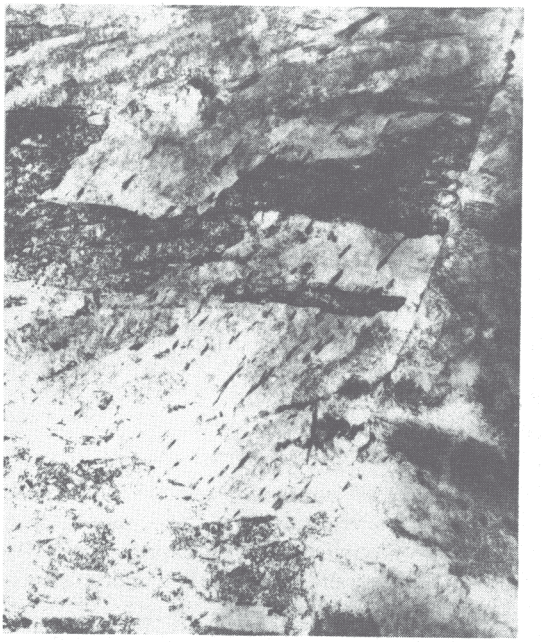

(b)

Fig. 3. Retained austenite at the platelet boundaries of lower bainite. (a) Retained austenite dark field image. (b) Corresponding bright field image.

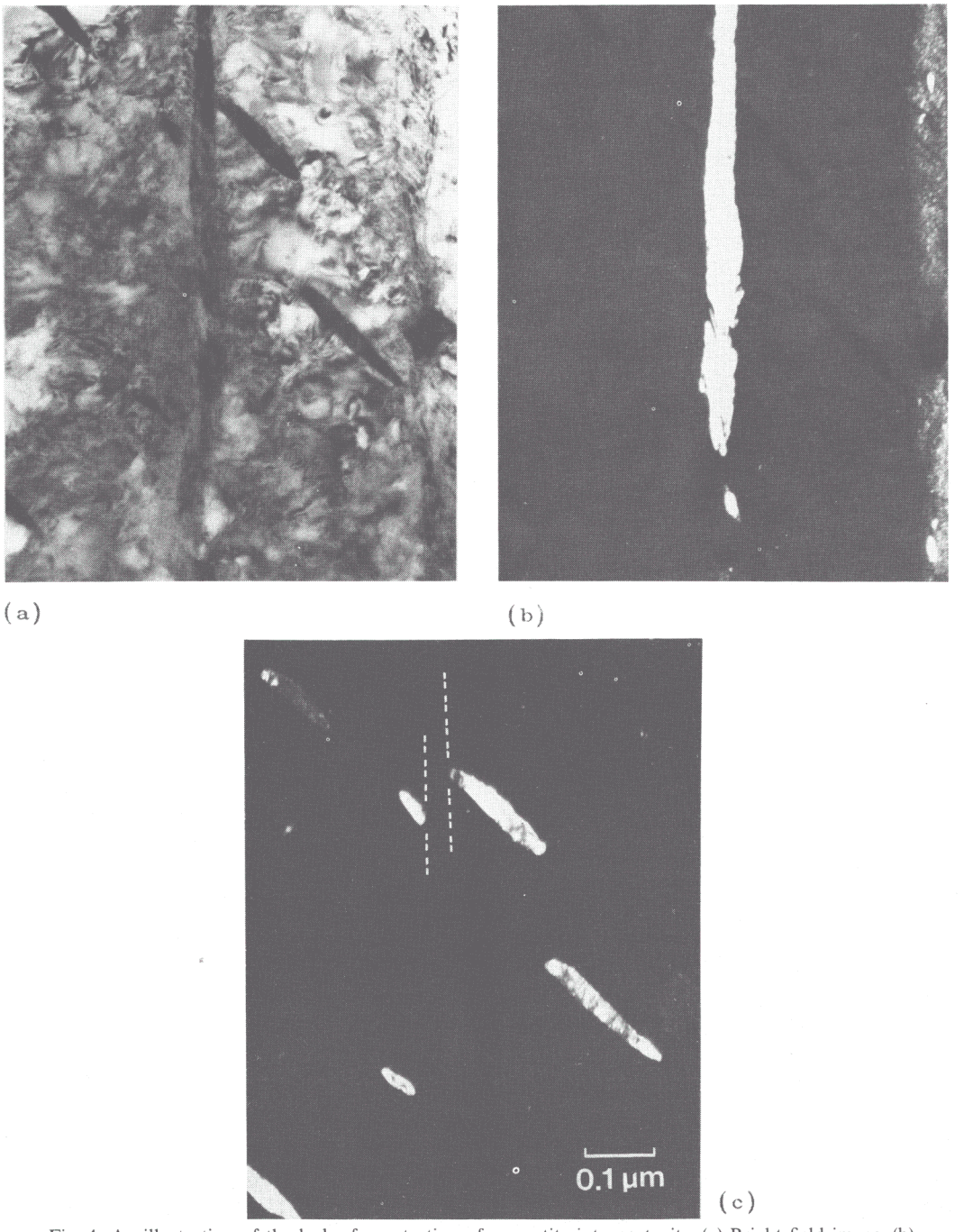

Fig. 4. An illustration of the lack of penetration of cementite into austenite. (a) Bright field image. (b) Retained austenite dark field image. (c) Cementite dark field image. The dashed lines indicate the position of the austenite/ferrite interface.

Nucleation and growth of carbides

The presence of substantial amounts of retained austenite in the microstructure allows current theories of interphase precipitation to be directly applied to the lower bainite transformation. The critical predictions of these theories amount to:

(a) The precipitate will attempt to minimise the interfacial energy by adopting an orientation variant which allows lattice matching with both the adjacent phases [25]. Accordingly, cementite nucleating at the austenite–ferrite interface is expected to exhibit the following three phase crystallography, which best satisfies the simultaneous lattice matching requirements:

(i) Kurdjumov–Sachs [26] related austenite and ferrite

$$[100]_\theta \| [0\bar{1}1]_\alpha \| [111]_\gamma$$
$$[010]_\theta \| [1\bar{1}\bar{1}]_\alpha \| [\bar{1}01]_\gamma.$$

(ii) Nishiyama–Wassermann [27] related cementite and ferrite

$$[100]_\theta \| [0\bar{1}1]_\alpha \| [111]_\gamma$$
$$[010]_\theta \| [1\bar{1}\bar{1}]_\alpha \sim 5^\circ \text{ from } [\bar{1}01]_\gamma$$

or

$$[100]_\theta \| [0\bar{1}1]_\alpha \| [111]_\gamma$$
$$[010]_\theta \| [\bar{1}\bar{1}\bar{1}]_\alpha \sim 5^\circ \text{ from } [0\bar{1}1]_\gamma.$$

The theory implies that if the predicted three-phase crystallography turns out to be unique, only one precipitate variant should be observed. Hence we note that two variants are expected if the Nishiyama–Wasserman orientation relationship operates between the austenite and ferrite.

(b) For the lower bainite transformation range, the penetration of cementite into austenite is expected to be *at least* an order of magnitude higher than that into ferrite [21]. The cementite at the interface is thus required to lie essentially within the austenite.

However, direct imaging of the austenite failed to reveal any carbide precipitation. Occasionally, carbide particles were found to impinge with the austenite–ferrite interface, and a few such cases were examined in detail. Figure 4 clearly shows that contrary to the expectations of interphase precipitation theory, the cementite is confined to the ferrite and hardly (if at all) penetrates the austenite. These observations strongly suggest that lower bainitic cementite nucleates from within supersaturated ferrite—the occasional impingements with the α/γ interface can be regarded as chance events.

When impingement does occur, it is not clear why the cementite does not subsequently continue to grow into the austenite. However, it is noted that the driving force for precipitation from supersaturated ferrite is expected to be higher than that associated with the decomposition of residual austenite—after all, austenite can comfortably accommodate a large amount of carbon in solid solution compared with supersaturated ferrite, whose equilibrium carbon content is below 0.03 wt.%. It seems therefore that not only do the carbides nucleate within the ferrite, but that the major part of their subsequent growth is accomplished by relieving carbon supersaturated ferrite. Confirmatory evidence was obtained by holding at the isothermal transformation temperature for a longer period (60 min at 435°C), when it was found that the residual austenite films had *diffusionally* decomposed. These films cannot decompose by further *displacive* bainite formation due to the 'incomplete reaction phenomenon' [10, 28, 29]. Essentially, what this implies is that the carbon content of the austenite becomes enriched to such an extent that displacive transformation becomes thermodynamically impossible. In accordance with the incomplete reaction phenomenon, the bainite transformation in the 0.3 C–4.08 Cr steel has been found to reach termination by 30 min at 435°C (Ref. [29]) and prolonged holding at this temperature only serves to induce the diffusional (reconstructive) decomposition of the carbon enriched retained austenite (Fig. 5). This directly demonstrates that the decomposition of austenite by the interphase precipitation of cementite is kinetically a very much slower process compared with precipitation involved in the formation of lower bainite (i.e. from supersaturated ferrite). This conclusion explains the fact that carbide precipitation does not accompany the upper bainite reaction in a silicon steel [3] even though cementite is found with the lower bainite in the same steel. It is generally accepted that upper bainitic carbide precipitation is a secondary event; the carbides nucleate at the α/γ interface and grow into the austenite so that the process is indeed one that can be described as interphase precipitation. Thus the carbide formation is expected to be very much slower for the silicon upper bainite and Bhadeshia and Edmonds [3] found that tempering at a higher temperature than the isothermal transformation temperature was necessary to induce the diffusional austenite decomposition to interphase carbides and ferrite.

Crystallography

To determine the crystallography of lower bainitic cementite, a set of five crystals were simultaneously and self-consistently analysed in order to avoid ambiguities and to enhance accuracy (the detailed analysis is presented in the Appendix). This set comprised two ferrite platelet groups, their two respective cementite variants and the parent austenite. The results are presented in Fig. 6. It was immediately found that the ferrite crystals could not be consistently indexed as Kurdjumov–Sachs (KS) variants, but were compatible with the Nishiyama–Wasserman (NW) orientation relationship. For each ferrite crystal, the cementite displayed a single variant of the Bagaryatski orientation relationship. We note that this is again inconsistent with interphase precipitation since it was earlier shown that two variants should form for the present NW austenite–ferrite orientation relationship. The final crystallography can be summarised as follows:

$[111]_\gamma = [011]_{\alpha_1}$	$[0\bar{1}1]_{\alpha_1} = [100]_{\theta_1}$	standard
$[1\bar{1}0]_\gamma = [100]_{\alpha_1}$	$[1\bar{1}\bar{1}]_{\alpha_1} = [010]_{\theta_1}$	variant
	$[211]_{\alpha_1} = [001]_{\theta_1}$	
$[1\bar{1}1]_\gamma = [0\bar{1}\bar{1}]_{\alpha_2}$	$[\bar{1}0\bar{1}]_{\alpha_2} = [100]_{\theta_2}$	
$[\bar{1}0\bar{1}]_\gamma = [100]_{\alpha_2}$	$[1\bar{1}\bar{1}]_{\alpha_2} = [010]_{\theta_2}$	
	$[\bar{1}\bar{2}1]_{\alpha_2} = [001]_{\theta_2}$	

This data unambiguously demonstrates that the three-phase crystallography deduced earlier for interphase precipitation does not operate since the cementite 'makes no effort' to match its lattice with the austenite. In neither case does the cementite bear a rational orientation relationship with respect to the austenite. The above three-phase crystallography was

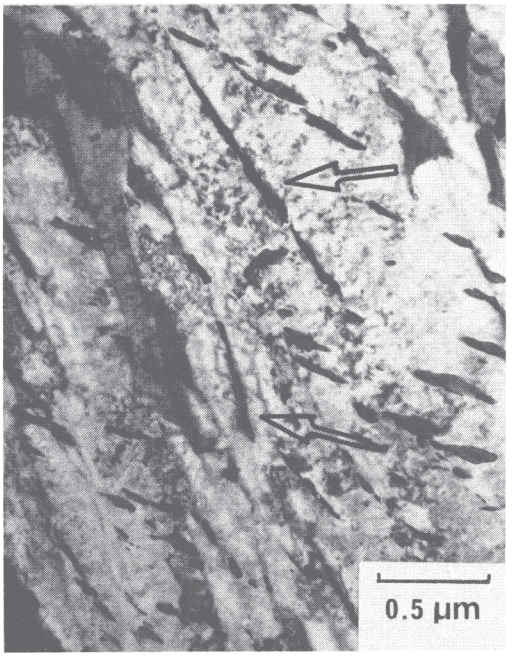

Fig. 5. Lower bainite following isothermal transformation at 435°C for the prolonged period of 30 min. The arrows indicate the positions of the cementite resulting from the diffusional decomposition of carbon-enriched residual austenite.

Fig. 6(a).

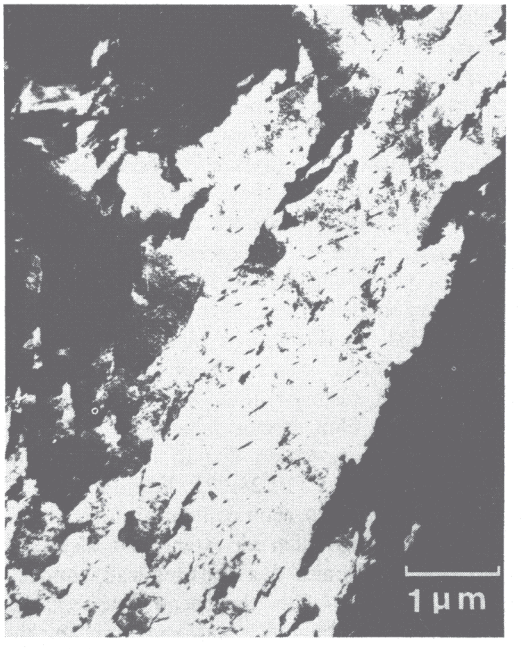

Fig. 6(b).

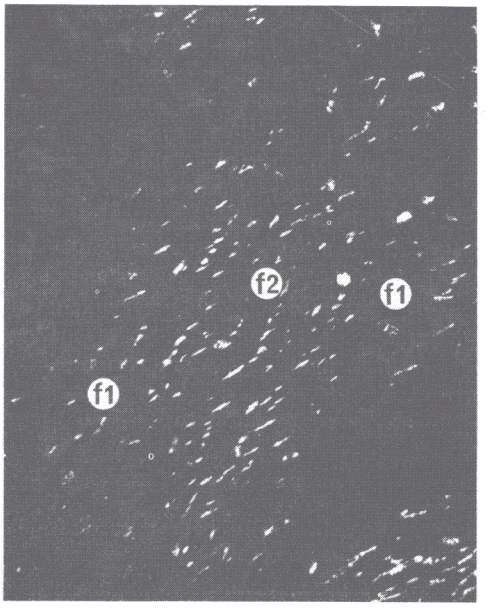

Fig. 6(c).

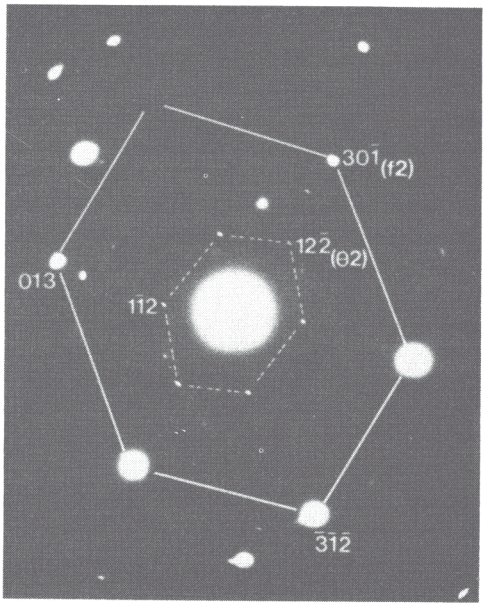

Fig. 6(d).

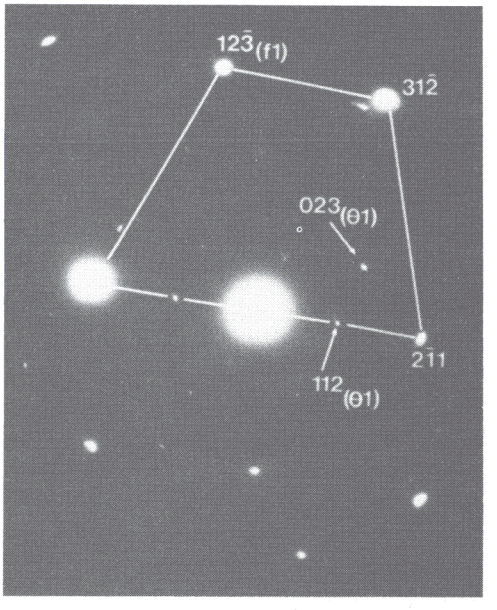

Fig. 6(e).

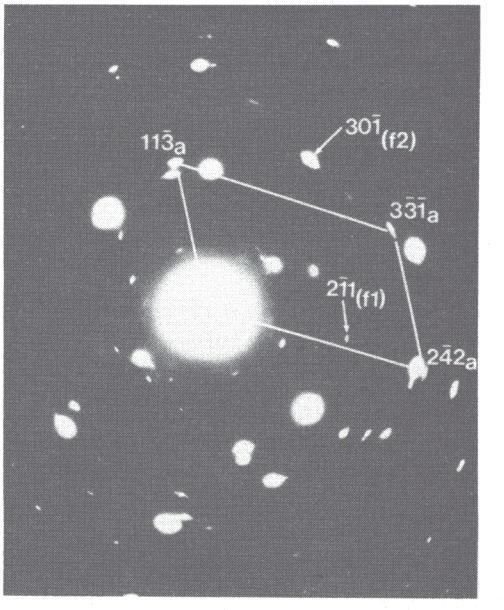

Fig. 6(f).

Fig. 6. Five crystal analysis, as referred to in the text. The subscripts a, f, θ refer to austenite, lower bainitic ferrite and cementite respectively. (a) Bright field image. (b) Dark field image of one of the bainitic ferrite variants (f_2). (c) Dark field image of θ_1 and θ_2 using the coincident 112_{θ_1} and $\bar{1}1\bar{2}_{\theta_2}$ reflections. (d)–(f) Corresponding selected area diffraction patterns.

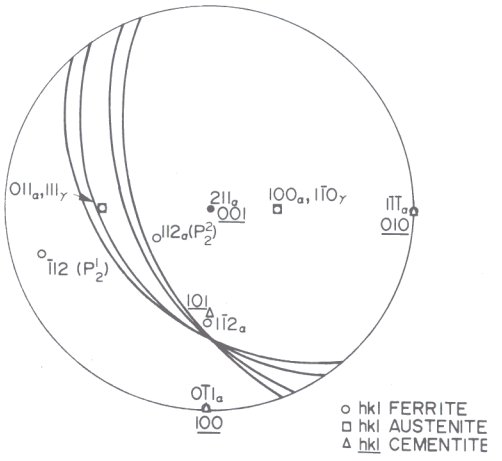

Fig. 7. Stereographic analysis of the crystallography of lower bainitic cementite. The intersection of the great circles defines the experimental habit plane. P_2^1 and P_2^2 refer to the planes of lattice invariant shear considered in the text.

verified for five sets of data. An interesting observation from all the data was that if the austenite and the particular variant of ferrite are indexed using the standard variant of the NW orientation relationship, the variant of cementite that forms is always specifically the same. Such regularity of three-phase crystallography bears a striking similarity to that of transformation twinning in martensite, where the operative twin variant is non-random, and has a unique relationship with the austenite–martensite crystallography [30].

Srinivasan and Wayman[4] suggested that lower bainitic cementite precipitation occurs on the $(112)_{\alpha_1}$ plane which, by the lattice correspondence of the standard variant, i.e.

$$^{f}C_b = \tfrac{1}{2}\begin{pmatrix} 1 & 1 & 0 \\ \bar{1} & 1 & 0 \\ 0 & 0 & 2 \end{pmatrix}$$

corresponds to the $(101)_\gamma$ plane in the austenite. Using detailed crystallography they further deduced that this was near the plane of lattice invariant shear for lower bainite in a high carbon steel, and suggested a close link between carbide precipitation and such slip shear.

However, in the present analysis (using the same standard correspondence), the precipitation plane as determined using self-consistent trace analysis which simultaneously utilised the experimentally determined cementite, ferrite and asutenite lattice orientations was found to be $(1\bar{1}2)_{\alpha_1} \sim (101)_{\theta_1}$†. The data are presented in Fig. 7, from which it is clear that the precipitate habit plane does not correspond to the plane of lattice invariant shear of [4]. It should be noted that the precipitation plane trace analysis of [4] was based only on the ferrite lattice.

It was further found that the great circle containing the pole of the habit plane (obtained using trace analysis with respect to both the ferrite and austenite lattices) had the indices $(0.6077, 0.4023, 0.6847)_{\alpha_1} \equiv (0.6282\ 0.\overline{2313}\ 0.\overline{7429})_\gamma$, and was inconsistent with the habit plane determined by [4] as $(0.2928, 0.7239, 0.6247)_\gamma$. It was therefore decided to examine the crystallography of the present lower bainite using the phenomenological theory of martensite. The calculations utilised a computer program due to Ledbetter and Wayman [32]. The following analysis (using the standard correspondence given earlier) was found to be compatible, within the limits of experimental error:

Input

p_2 = Plane of lattice invariant shear = $(011)_\gamma \equiv (\bar{1}12)_\alpha$.

d_2 = Direction of lattice invariant shear = $[0\bar{1}1]_\gamma \equiv [1\bar{1}1]_\alpha$.

Principal distortions = 1.126435, 1.126435, 0.796510.

Results

M_1 = Magnitude of shape deformation = 0.229217.

M_2 = Magnitude of lattice invariant deformation = 0.244843.

P_1 = Habit Plane = $(0.761318\ 0.169269\ 0.625893)_\gamma$

Angle between $(111)_\gamma$ and $(011)_{\alpha_1}$ = 0.67°.

Angle between $[\bar{1}01]_\gamma$ and $[\bar{1}\bar{1}1]_{\alpha_1}$ = 6.51°.

It should be noted the P_1 lies only $1\frac{1}{2}°$ from the experimentally determined great circle (given earlier) which must contain the habit plane pole, and the Nishiyama–Wasserman orientation relationship is also approximately consistent with the predicted results. Furthermore, the value of M_1 is reasonable when compared with that of martensite [33].

Hence we still find that the plane of cementite precipitation i.e. $(1\bar{1}2)_{\alpha_1}$ does not correspond to the plane of lattice invariant shear. It is thus proposed that the precipitation of cementite is not related to the lattice invariant shear itself, but to the relief of the overall strain energy associated with the shape deformation of lower bainite. The formation of cementite necessitates the flow of vacancies due to the difference in specific volume relative to ferrite. Clearly, the presence of any elastic strains in the ferrite must influence such flow, in a manner such that the strains are somewhat relieved. Thus the appearance not only of a single variant, but of a variant that is specifically related to the austenite–ferrite crystallography is not surprising, since a unique strain tensor will be associated with a given ferrite variant. The observation [34] that carbide precipitation modifies the surface relief of lower bainite supports this conclusion, particularly since freshly formed plates (apparently without carbide precipitation) exhibit perfect invariant-plane strain relief. Furthermore, Christian [35] points out

† Shackleton and Kelly [22, 23] showed that the plane of precipitation of cementite from ferrite is $\{101\}_\theta \sim \{112\}_\alpha$. Such a relation is also consistent with the habit plane containing the direction of maximum coherency between the θ and α lattices, i.e. $\langle 010\rangle_\theta \| \langle 11\bar{1}\rangle_\alpha$ (Ref. [31]).

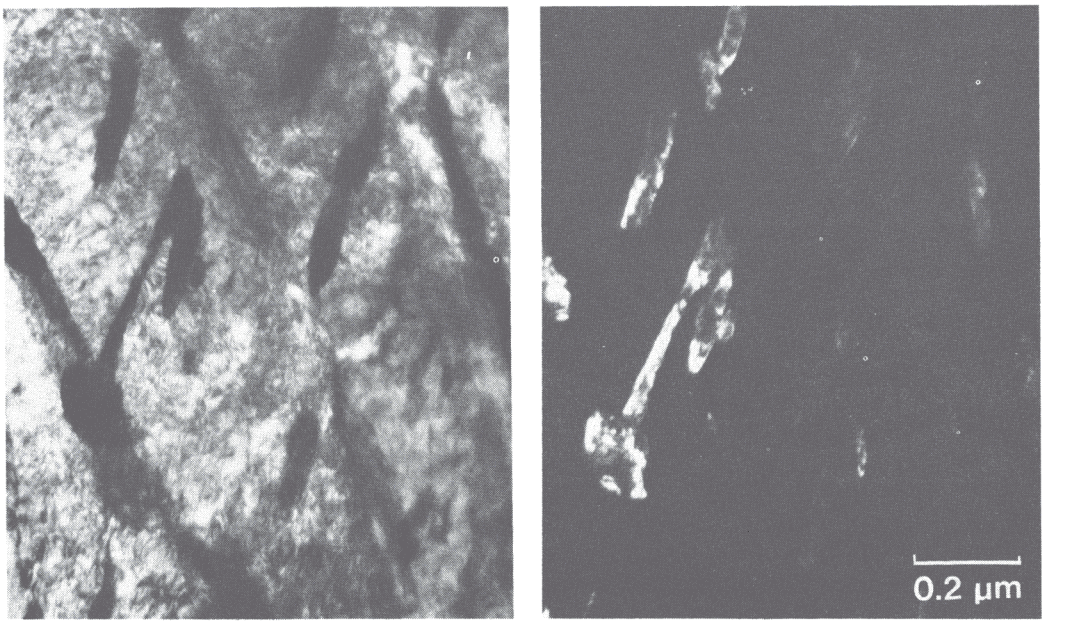

(a) (b)

Fig. 8. The nature of carbide precipitation at an impingement between an internal carbide and the bainitic ferrite/prior austenite interface. (a) Bright field image. (b) Corresponding cementite dark field image.

that any substitutional diffusion reactions should destroy the lattice correspondence and its associated strain energy. In this sense, the post-bainitic precipitation of cementite can be regarded as a diffusional reaction that relieves the transformational strain energy to some extent.

The crystallography of interphase carbide precipitation due to the diffusional decomposition of the films of residual austenite was examined by holding specimens at the isothermal transformation of 435°C for the prolonged period of 60 min. It was noticed that when such precipitation occurred at the sites of impingement of internal carbides with the α/γ interface, the austenite decomposed into cementite of the same orientation (although not the same morphology) as the internal carbides (Fig. 8). It is evident that the impinging carbide must have aided the nucleation of cementite in such cases. However, in a case where the decomposition of residual austenite seemed to have occurred as an independent event, two variants of cementite were detected, neither of which were equivalent to the internal carbide variant (Fig. 9). Tentatively, this is *consistent* with the interphase precipitation theory, although the lack of austenite prevented more detailed analysis.

The transition from upper to lower bainite

Pickering [17] systematically studied the variation of the transition temperature between upper and lower bainite as a function of carbon content in steels containing 0.5Mo plus boron or 1.0Cr–0.5Mo plus boron. His data points are reproduced in Fig. 10. He suggested that upper bainite gives way to lower bainite when the rate of carbon diffusion away from the ferrite is too slow so that the supersaturated ferrite has to precipitate carbide for continued growth. In order to explain the apparent initial rise (0–0.4C) in transition temperature with an increase in carbon content (Fig. 10) he proposed that it gets progressively difficult to remove carbon from supersaturated bainitic ferrite as the alloy carbon content increases since the concentration gradients in austenite will become shallower. Thus it becomes easier to precipitate carbides from ferrite as the alloy carbon content increases, so that the transition temperature rises.

However, it has been demonstrated [36] that the removal of carbon from ferrite is orders of magnitude faster compared with the levelling of diffusion gradients in austenite. Additionally, Pickering's model implies that the only difference between upper and lower bainite is that the latter contains internal carbides whereas definite morphological differences have been demonstrated to exist between these two reactions [3]. It is also inconsistent with the fact that upper and lower bainite often form at the same temperature in a given steel [3, 17]. It is therefore suggested that the transition temperature must reflect a change in morphology and that the apparent initial rise in the transition temperature with increasing carbon may be due to the difficulty of avoiding the upper bainite reaction during the quench to the isothermal transformation temperature. In essence, this amounts to a hardenability problem, but with respect to interference from the upper bainite transformation in low carbon steels. This hypothesis is further supported by the fact that the apparent peak in the transition curve is shifted to considerably lower carbon levels with an increase in alloy content [18]. The latter would be expected to mitigate the hardenability problem.

In Fig. 10, comparison of Pickering's data with the

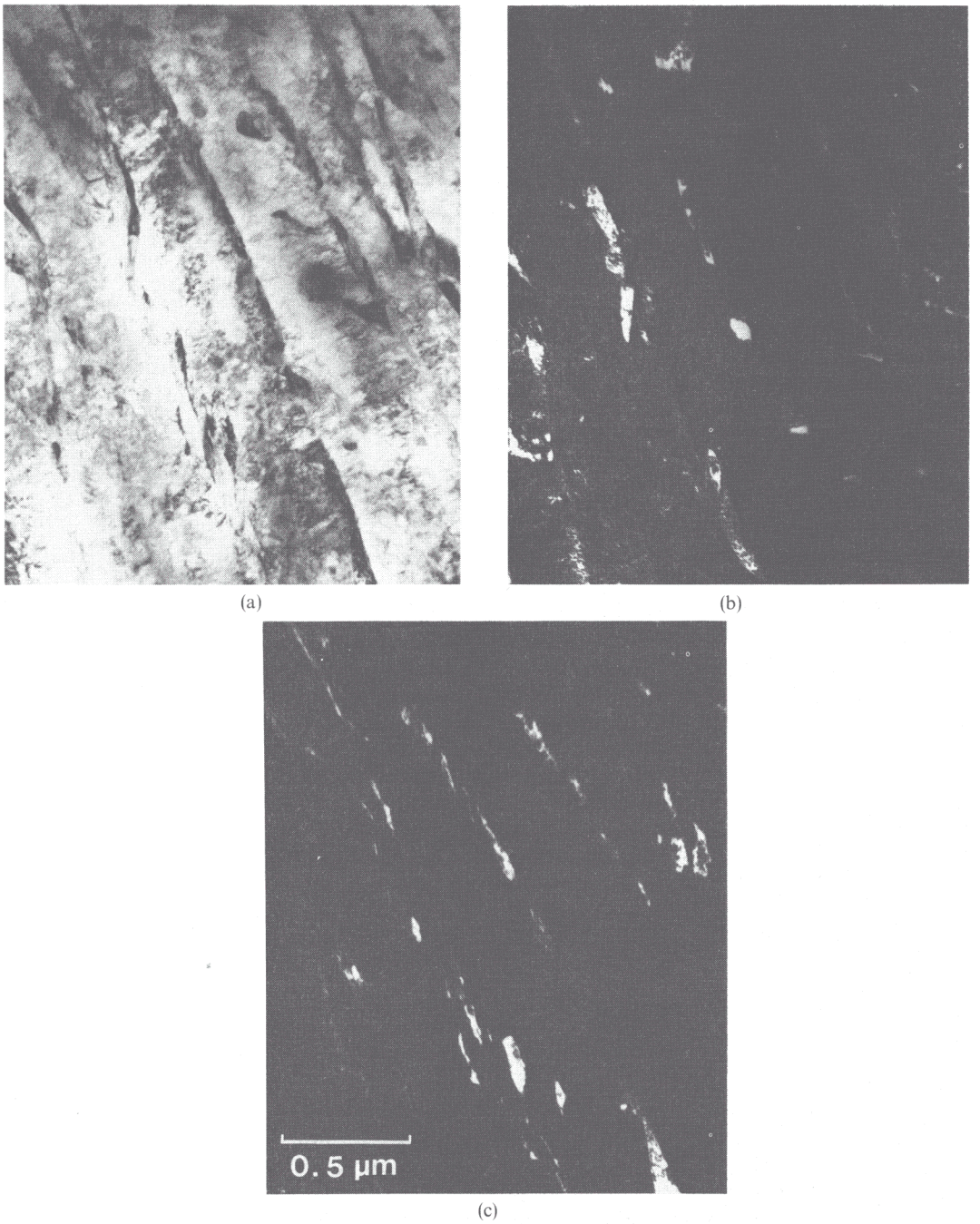

Fig. 9. The nature of interphase precipitation following the independent nucleation of cementite during the diffusional decomposition of residual austenite. (a) Bright field image. (b) θ_1 dark field image. (c) θ_2 dark field image.

bainite start (B_s) and martensite start (M_s) lines given by Steven and Haynes [37] suggests that the transition temperature between upper and lower bainite (or the lower bainite start temperature) should also vary in a similar manner. Indeed, if the low carbon data (i.e. first two points) is ignored due to the above mentioned difficulties, the majority of the points position neatly between the B_s and M_s lines. In fact, a decrease in the lower bainite start temperature (LB_s) with increasing carbon content is expected on thermodynamic grounds since the driving force (for a given transformation temperature) for the displacive decomposition of austenite decreases with increasing carbon content [38]. If it is assumed that the lower bainite reaction requires a certain build-up of driving force before the onset of transformation, as is approximately the case for martensite [38] and for upper bainite [28], then it follows that the transition temperature must decrease with increasing carbon content.

The approximately constant transition temperature beyond a carbon concentration of about 0.8 wt.% can

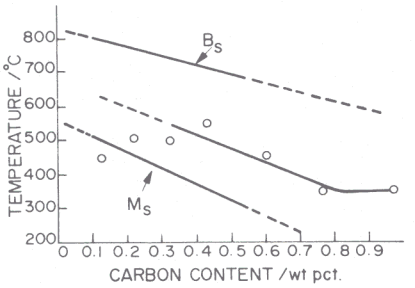

Fig. 10. The lower bainite start temperature (data due to Pickering) in relation to the B_s and M_s temperatures.

be rationalised if it is assumed that prior carbide formation occurs in hypereutectoid steels, so that the carbon content of the austenite is locally (or otherwise) reduced to a constant level (given by the eutectoid composition) before the formation of bainitic ferrite. Primary cementite precipitation is indeed found in hypereutectoid steels [39], where the so-called inverse bainite occurs.

The choice between ϵ-carbide and cementite

The following table list shows that the steels in which lower bainitic epsilon carbide has been positively identified invariably have a high carbon content.

Steel composition: C	Si	Mn	Ni	Cr	Mo	V	Ref.
0.95	0.22	0.60	3.27	1.23	0.13	—	[5]
0.60	2.00	0.86	—	0.31	—	—	[5]
1.00	0.36	—	0.20	1.41	—	—	[5]
0.58	0.35	0.78	—	3.90	0.45	0.9	[5]
1.00	2.15	0.36	—	—	—	—	[6, 7]
0.54	1.87	0.79	—	0.30	—	—	[9]
0.60	2.00	0.86	—	0.31	—	—	[8]
0.60	2.00	—	—	—	—	—	[10]

However, as was noted earlier, only cementite is found in a 0.43C–3Mn–2Si steel [3] and in the present steel. These differences in behaviour need rationalisation. Bhadeshia and Edmonds [3] originally suggested that the lack of epsilon carbide in the 0.43C alloy steel may be due to the presence of the substantial amount of manganese. However, as Hehemann [40] has pointed out, epsilon can be found on tempering the martensite in the same steel [41], and, in any case, this would not explain the lack of epsilon carbide in the present chromium steel.

Kalish and Cohen [16] have shown that it is energetically favourable for carbon atoms to remain segregated at dislocations compared with their presence in the epsilon carbide lattice. Hence, if the dislocation density is high (as is the case for bainites–Ref. [3]), sufficient carbon can be captured by the dislocations so that the epsilon carbide precipitation stage is entirely missed out in the tempering sequence. In such cases cementite precipitation occurs directly. Kalish and Cohen estimate that a dislocation density of 2×10^{12} cm^{-2} will prevent epsilon carbide precipitation in steels of up to 0.20 wt.% carbon.

Considering the case for bainite, following the formation of supersaturated bainite, two competitive reactions begin. These are the processes of carbon partitioning into residual austenite and the precipitation of carbides within the ferrite. Hence the effective amount of carbon available for precipitation is reduced. Judging from available data [3, 6–10], it seems that sufficient carbon for epsilon formation during the bainite reaction is only available when the average carbon content of the steel is above approximately 0.55 wt.%. Hence the theory of Kalish and Cohen seems to explain the various carbides observed in lower bainite. The basic steel composition may have some effect, but this has not been systematically studied and is not considered further.

GENERAL SUMMARY

It has been shown that lower bainitic cementite nucleates and grows within supersaturated ferrite. Furthermore, such precipitation has been found to be strongly inconsistent with the concept of interphase precipitation.

Crystallographic determinations indicated that the lattice invariant shear associated with lower bainite formation may not be responsible for the development of a single carbide variant. It has been suggested that the strain energy associated with a platelet of lower bainite stimulates the development of the particular carbide variant that is compatible with the relief of this strain energy.

The transition temperature from upper to lower bainite has been tentatively rationalised on thermodynamic grounds and within the context of the B_s and M_s temperatures.

It has been shown that the appearance of epsilon carbide in some lower bainites but cementite in others can be understood in terms of an available martensite tempering theory of Kalish and Cohen [16].

The present results are consistent with the displacive formation of supersaturated bainitic ferrite. However, the extent of this supersaturation is not clear since some carbon must partition into the residual asutenite during transformation in order to provide the necessary driving force for a displacive reaction.

Acknowledgements—The author is grateful to the Science Research Council for a Research Fellowship and to RARDE, Fort Halstead for kindly providing the alloy used in this investigation. Thanks are due to Professor R. W. K. Honeycombe for the opportunity to work in his Alloy Steels Research Group and for the provision of laboratory facilities.

REFERENCES

1. K. J. Irving and F. B. Pickering, *JISI* **188,** 101 (1958).
2. G. R. Speich, *The Decomposition of Austenite by Diffusional Processes*, p. 353. Interscience, New York (1962).

3. H. K. D. H. Bhadeshia and D. V. Edmonds, *Metall. Trans.* **10A,** 1895 (1979).
4. G. R. Srinivasan and C. M. Wayman, *Acta Metall.* **16,** 609 (1968).
5. S. J. Matas and R. F. Hehemann, *Trans. AIME* **221,** 179 (1961).
6. J. Deliry, *Mem. Sci. Rev. Metall.* **62,** 527 (1965).
7. J. Pomey, *Mem. Sci. Rev. Metall.* **63,** 2 (1966).
8. J. M. Oblak and R. F. Hehemann, *Transformation and Hardenability in Steels*, Symposium by the Climax Molybdenum Co., Ann Arbor, p. 15 (1967).
9. Der Hung Huang and G. Thomas, *Metall. Trans.* **8A,** 1661 (1977).
10. R. F. Hehemann *Phase Transformations*, ASM, Metals Park, Ohio, p. 397 (1970).
11. W. S. Owen, *Trans. ASM* **46,** 812 (1954).
12. J. Gordine and I. Codd, *JISI*, **207.1,** 461 (1969).
13. R. M. Hobbs, G. W. Lorimer and N. Ridley, *JISI* **210.2,** 757 (1972).
14. G. R. Speich, *Trans. AIME* **245,** 2553 (1969).
15. M. Cohen, *J. Inst. Metals, Spec. Supp.* **9,** 103 (1968).
16. D. Kalish and M. Cohen, *Mater. Sci. Engng* **6,** 156 (1970).
17. F. B. Pickering, *Transformation and Hardenability in Steels*, Symposium by the Climax Molybdenum Co., Ann Arbor, p. 109 (1967).
18. A. M. Llopis, Ph.D. Thesis, referred to in E. R. Parker, *Metall. Trans.* **8A,** 1025 (1977).
19. R. F. Hehemann, K. R. Kinsman and H. I. Aaronson, *Metall. Trans.*, **3,** 1077 (1972).
20. R. W. K. Honeycombe, *Metall. Trans.* **7A,** 915 (1976).
21. H. I. Aaronson, H. R. Plichta, G. W. Franti and K. C. Russell, *Metall. Trans.* **9A,** 363 (1978).
22. D. N. Shackleton and P. M. Kelly, *Acta Metall.* **15,** 979 (1967).
23. D. N. Shackleton and P. M. Kelly, *ISI, London Spec. Rep.* **93,** p. 126 (1965).
24. Y. A. Bagaryatski, *Dokl. Akad. Nauk SSSR* **73,** 1161 (1950).
25. P. R. Howell, J. V. Bee and R. W. K. Honeycombe, *Metall. Trans. A*, in press (1980).
26. G. V. Kurdjumov and G. Sachs, *Z. Phys.* **64,** 325 (1930).
27. Z. Nishiyama, *Sci. Rep. Tohoku Univ.* **23,** 325 (1934).
28. H. K. D. H. Bhadeshia and D. V. Edmonds, *Acta Metall.* In press.
29. H. K. D. H. Bhadeshia, Unpublished Research, University of Cambridge.
30. J. W. Christian, *The Theory of Transformations in Metals and Alloys.* Pergamon Press, Oxford, (1965).
31. K. W. Andrews, *Acta Metall.* **11,** 939 (1963).
32. H. M. Ledbetter and C. M. Wayman, *Mater. Sci. Engng* **7,** 151 (1971).
33. G. R. Srinivasan and C. M. Wayman, *Acta Metall.* **16,** 621 (1968).
34. H. M. Clark and C. M. Wayman, *Phase Transformations*, ASM, Metals Park, Ohio, p. 59 (1970).
35. J. W. Christian, *Decomposition of Austenite by Diffusional Processes*, Interscience, p. 371 (1962).
36. H. I. Aaronson and K. I. Kinsman, Discussion to Ref. [8].
37. W. Steven and A. J. Haynes, *JISI*, **183,** 349 (1956).
38. L. Kaufmann and M. Cohen, *Prog. Metal Phys.* **7,** 165 (1958).
39. M. Hillert, *Jernkontorets Ann.* **141,** 757 (1957).
40. R. F. Hehemann, private communication (1979).
41. H. K. D. H. Bhadeshia and D. V. Edmonds, *Metal Sci.* **2,** 325 (1979).

APPENDIX

It was found that in order to achieve consistent indexing of the diffraction patterns involved in the five crystal analysis, the α–γ orientation relationship could not be taken to be of the Kurdjumov–Sachs type. For instance, if α_1 and γ are indexed as

$$(111)_\gamma \| (011)_{\alpha_1}$$
$$[\bar{1}01]_\gamma \| [\bar{1}\bar{1}1]_{\alpha_1} \quad \text{(standard variant)}$$

then α_2 cannot also be indexed as a K–S variant. This is because the operative $[\bar{5}43]_\gamma$ zone axis cannot be transformed to an α zone axis that is near or equivalent to a $\langle 1\bar{9}3\rangle_{\alpha_2}$ zone axis using any of the 24 crystallographically independent K–S transformation matrices, such that the corresponding $[1\bar{2}1]_\gamma$ falls near the $\langle 013\rangle_{\alpha_2}$ which lies in the $\langle 193\rangle_{\alpha_2}$ zone, as is experimentally observed.

Furthermore, the K–S relationship (standard variant) requires that $(1\bar{2}1)_\gamma \| (2\bar{1}1)_{\alpha_1}$ whereas examination of Fig. 6 shows that this is not the case.

However, both the α variants can be consistently indexed using the Nishiyama–Wassermann orientation relationship, the specific variants being described by the following matrix representations:

$$(hkl)_{\alpha_1} = (hkl)_\gamma \begin{pmatrix} 0.70711 & 0.69692 & 0.11957 \\ -0.70711 & 0.69692 & 0.11957 \\ 0 & -0.16910 & 0.98560 \end{pmatrix}$$

$$(hkl)_{\alpha_2} = (hkl)_\gamma \begin{pmatrix} 0.70711 & -0.69692 & -0.11957 \\ 0 & -0.16910 & 0.98560 \\ 0.70711 & -0.69692 & -0.11957. \end{pmatrix}$$